

# Design of a Compact Stacked Yagi with a Novel Slotted Reflector and a Ladder-Like Director for Bandwidth Enhancement

Li Jiang\*, Fu-Shun Zhang, and Fan Zhang

**Abstract**—A compact stacked Yagi antenna is proposed with bandwidth enhancement in this paper. To reduce the size of the antenna and simultaneously improve the front-to-back ratio (FTBR), a reflector, modified with six slots, two  $\lambda_0/4$  meanderline-shaped slots and four straight short slots, is employed. Furthermore, a ladder-like director is designed to overcome the mismatch loss caused by the diminution of the height between the reflector and driven dipole. As shown in both simulation and measurement, the proposed compact Yagi antenna can achieve a compact size of  $0.55\lambda_0 \times 0.55\lambda_0 \times 0.08\lambda_0$ , a  $|S_{11}| \leq -10$  dB bandwidth of 17.2% and an FTBR of 22 dB at 2.2 GHz. The acceptable results make the proposed Yagi antenna a good candidate for applications where compact size and wide bandwidth are needed.

## 1. INTRODUCTION

Vertically multilayer-stacked Yagi-Uda antennas have attracted interest in various electromagnetic application areas for their high gain and easy fabrication [1]. However, the bulky structure and narrow impedance bandwidth (Here, the impedance bandwidth mentioned is the range of frequencies for which  $|S_{11}| \leq -10$  dB, i.e., the  $50\ \Omega$  impedance bandwidth.) have limited their applications. Especially in aircraft wideband communication, to reduce the influence of aerodynamic, the wideband Yagi-Uda antennas with low profile are desired.

A Yagi antenna is composed of a driver element, a reflector and several directors. To reduce the whole size and enhance the impedance bandwidth, many efforts have been made, such as the diminution of the distance between elements, utilization of a wide-impedance bandwidth feeding structure, and introduction of parasitic elements. As a classic topic, when the elements of a Yagi antenna get closer, the radiation resistance drops dramatically, which creates mismatch loss and narrow impedance bandwidth [2, 3]. Furthermore, while reducing the profile and size of the vertically multilayer-stacked Yagi-Uda antenna, caused by the edge diffraction, its front-to-back ratio (FTBR) becomes small as well [3]. Therefore, much more attention should be taken to the study on compact stacked Yagi antennas with relatively wide impedance bandwidth and high FTBR.

In recent years, various designs have been presented to achieve this goal. Generally, there are two main ways. One way is to change the structure of the driver element by increasing its volume for increasing the radiation resistance [4–6]. By replacing a straight dipole with a horizontally positioned multi-folded structure, a three-element folded Yagi antenna [4] working at 104.5 MHz achieves a distance of  $0.02\lambda_0$  (where  $\lambda_0$  is the wavelength at the operating frequency in free space) between the driver and reflector within an impedance bandwidth of 1%. A slot structure combined with multilayered topology has been applied to obtain a low antenna profile of  $0.18\lambda_0$  at 3.475 GHz with an FTBR of 13 dB and an operating impedance bandwidth of 11.8% [5]. The other way is to tune the phase of the electric field reflected from the ground plane by introducing artificial surfaces as reflectors, for

---

Received 16 May 2017, Accepted 15 August 2017, Scheduled 24 August 2017

\* Corresponding author: Li Jiang (15829775859@163.com).

The authors are with the Science and Technology on Antenna and Microwave Laboratory, Xidian University, Xi'an, Shaanxi 710071, China.

instance, electromagnetic band gap (EBG) [7, 8] and split-ring resonators (SRR) [9]. By applying the EBG ground of  $0.9\lambda_0 \times 0.9\lambda_0$ , a horizontally placed dipole [7] has achieved a height of  $0.07\lambda_0$  with an impedance bandwidth of 16%. A dipole [9] placed above an SRR based ground surface of  $0.5\lambda_0 \times 0.5\lambda_0$  has obtained a height of  $0.05\lambda_0$  over an impedance bandwidth of 0.1%. Nevertheless, its FTBR is less than 4 dB, which is difficult to meet the requirement of many wireless applications, where space constraint is demanded.

Recently, a straight parasitic strip [2] is placed closely and horizontally above a perfect electrical conductor ground plane, which makes the horizontal dipole attain a height of  $0.05\lambda_0$ , an impedance bandwidth of 0.6% and an FTBR of 17 dB.

However, the above antennas cannot solve the damage caused by the lower profile. All of these reported antennas bring either narrow impedance bandwidth ( $< 1\%$ ) or high profile ( $> 0.1\lambda_0$ ). None of them can achieve a good low profile as well wideband property.

In this paper, a compact stacked 3-elements Yagi antenna is proposed with a size of  $0.55\lambda_0 \times 0.55\lambda_0 \times 0.08\lambda_0$ , a relatively wide impedance bandwidth of 17.2% and an FTBR of 22 dB at 2.2 GHz. A reflector, modified with six slots, two  $\lambda_0/4$  meanderline-shaped slots and four straight short slots, is employed to reduce the profile of the antenna and simultaneously improve the FTBR with a compact size. To solve mismatch loss caused by the decrease of the distance between the reflector and driven dipole, a ladder director is designed. By properly tuning the length and the overlapping region of the ladder director, the impedance bandwidth of the proposed antenna is improved to 17.2%. Moreover, the driven printed dipole is simply fed by a coaxial line, further contributing to the compactness of the proposed Yagi antenna without balun. All these good performances make the proposed Yagi antenna more favorable for aircraft wideband communication where wide-bandwidth, low profile and compact size are needed.

## 2. ANTENNA DESIGN

The structure of the proposed Yagi antenna is illustrated in Fig. 1. It consists of three layers, and all Cu foil elements are printed on an F4BM-2 substrate with a thickness of  $9\ \mu\text{m}$ . The F4BM-2 substrate

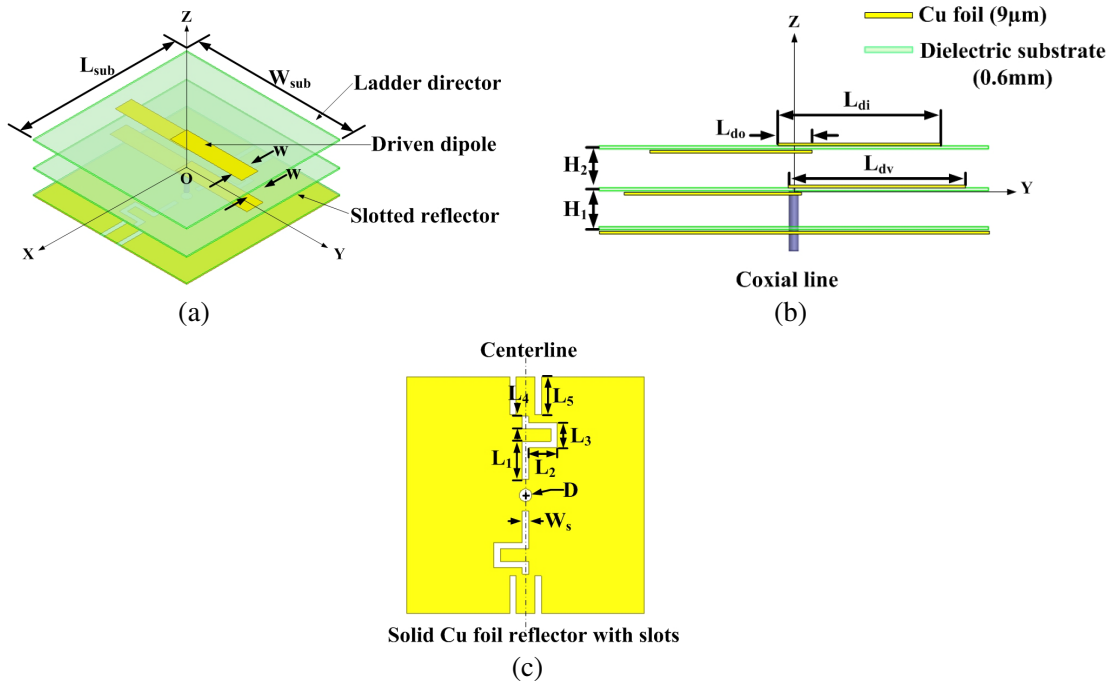


**Figure 1.** The structure of the low profile Yagi antenna. (a) 3D view; (b) side view; (c) solid Cu foil reflector with slots.

**Table 1.** List of all the dimensional parameters for the proposed Yagi antenna in Fig. 1.

<b>Parameters</b>	$W_{\text{sub}}$	$L_{\text{sub}}$	$w$	$L_{\text{di}}$	$L_{\text{do}}$	$L_{\text{dv}}$	$H_1$	$H_2$
<b>Values (mm)</b>	<b>75</b>	<b>75</b>	<b>8</b>	<b>34</b>	<b>4</b>	<b>35</b>	<b>6</b>	<b>6</b>
<b>Parameters</b>	$L_1$	$L_2$	$L_3$	$L_4$	$L_5$	$W_s$	$D$	
<b>Values (mm)</b>	<b>11</b>	<b>8</b>	<b>7</b>	<b>4</b>	<b>11</b>	<b>2</b>	<b>3</b>	

used for the simulation and antenna fabrication has a relative permittivity of 2.65, loss tangent of 0.002, and thickness of 0.6 mm. The ladder director lies on the first substrate. As shown in Fig. 1(b). The traditional straight director is replaced by two ladder-like segments, which are printed on the two sides of the first substrate, respectively. The driven dipole is simply fed by a 50- $\Omega$  coaxial line and located at both sides of the second layer. For not connecting to the coax-feed line, an isolated hole is inserted in the middle of the third substrate as well as the reflector. Meanwhile, the reflector is at the bottom of the third layer with six slots cut in it, two  $\lambda_0/4$  meanderline-shaped slots and four straight short slots. The centerline of the slots is oriented orthogonally to the axis of the driven dipole. For wideband property, the distance  $H_1$  between the reflector and the driven dipole is  $0.04\lambda_0$ , and the distance  $H_2$  between the director and the driven dipole is the same, i.e.,  $H_1 = H_2 = 0.04\lambda_0$ . Detailed dimensions of the proposed low profile Yagi antenna are listed in Table 1.

## 2.1. Operating Principle of Compact Size

In this section, the operating principle of the proposed compact stacked Yagi antenna with a high FTBR is presented. For the stacked Yagi antenna, a practical way of achieving low profile property is to reduce the distance between the reflector and the driven dipole. By reflecting the electric fields radiated from the dipole, the reflector limits the pattern of the Yagi and, more importantly, affects the front-to-back ratio (FTBR).

Therefore, to study the effects of the reflector and the height  $H_1$  between the driven dipole and reflector on FTBR, four cases are depicted in Fig. 2. Moreover, their simulated FTBRs are listed in Table 2. First, a traditional two-elements Yagi antenna with a height of  $H_1 = 0.2\lambda_0$  and reflector size of  $\lambda_0 \times \lambda_0$  is given. A good FTBR of 16 dB is obtained since the electric fields radiated from the dipole and reflected by the reflector are in phase on its boresight direction [2]. Second, the height  $H_1 = 0.2\lambda_0$  is reduced to  $H_1 = 0.04\lambda_0$ . The FTBR is enlarged to 20 dB. The reason for this is that the wave of polarization parallel to the reflector disappears on the surface of the reflector, which greatly compresses the beam width. Then, the third case is to shrink the size of the reflector while keeping  $H_1 = 0.04\lambda_0$ . As expected, with a size of  $0.5\lambda_0 \times 0.5\lambda_0$ , backward radiation is generated in the direction of the smaller reflector due to the edge diffraction. The FTBR decreases tremendously from 20 dB to 8 dB. Last, instead of the aforesaid reflector, a perfect electric ground in a size of  $0.55\lambda_0 \times 0.55\lambda_0$  and height of  $H_1 = 0.04\lambda_0$  modified with six slots is proposed as shown in Fig. 1(c). Its corresponding FTBR achieves a notable improvement.

**Table 2.** Simulated FTBR of four cases.

	$H_1$	Reflector size	FTBR (dB)
<b>Case 1</b>	$0.2\lambda_0$	$\lambda_0 \times \lambda_0$	<b>16</b>
<b>Case 2</b>	$0.04\lambda_0$	$\lambda_0 \times \lambda_0$	<b>20</b>
<b>Case 3</b>	$0.04\lambda_0$	$0.5\lambda_0 \times 0.5\lambda_0$	<b>8</b>
<b>Case 4 (proposed)</b>	$0.04\lambda_0$	$0.55\lambda_0 \times 0.55\lambda_0$	<b>19</b>

This phenomenon indicates that a slot-modified reflector can be utilized to suppress the radiation of the back lobe [10, 11]. Furthermore, to fully understand the operating principles, current distributions on the latter antenna at the frequency of 2.2 GHz are shown in Fig. 3. With the effect of the slots,

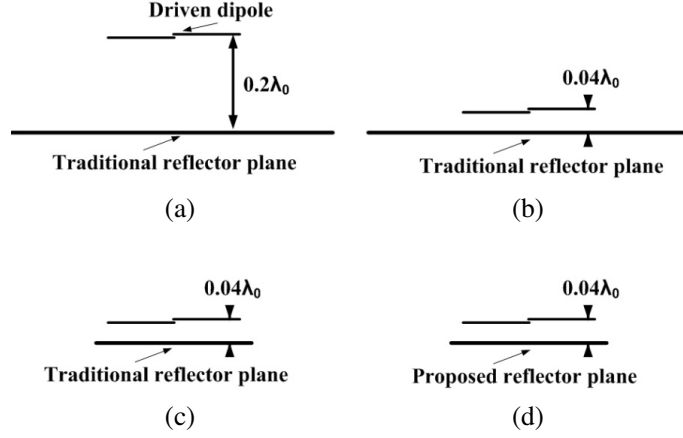


**Figure 2.** Four cases with varied height and different reflector for comparison. (a) Case 1. (b) Case 2. (c) Case 3. (d) Case 4.

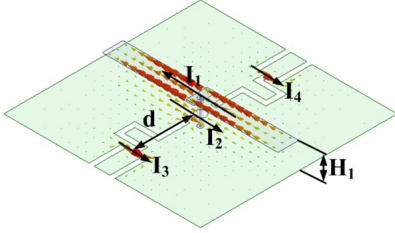


**Figure 3.** Simulated current distributions on the driven dipole and slot-modified reflector at 2.2 GHz.

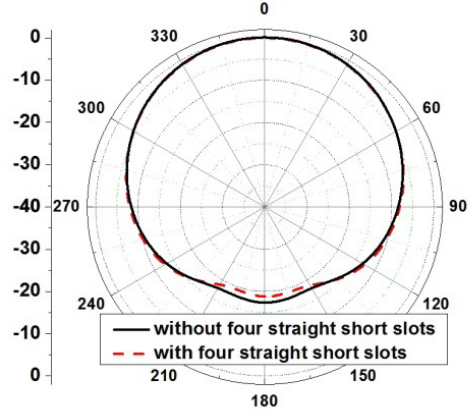


**Figure 4.** Simulated radiation patterns with/without the four straight short slots at 2.2 GHz.

induced currents ( $I_2, I_3, I_4$ ) on the slot-modified reflector and exciting currents ( $I_1$ ) on the driven dipole can be described as a four-element dipole array. Ignoring the mutual interaction, our emphasis is put on whether or not such an equivalent model can achieve high FTBR values along  $z$ -axis. Taking  $I_1$  as the reference, its amplitude is set to 1, and its phase is set to  $0^\circ$ . As shown in Fig. 3,  $I_2$  has an out-of-phase  $\pi$  and an amplitude  $A$ ;  $I_3$  and  $I_4$  have the same amplitude and phase, which can be set to  $B$  and  $\alpha$ , respectively. Using the pattern analysis in the normalized directivity of this equivalent model [11], the directivity in the  $xoz$ -plane and  $yo z$ -plane can be achieved.

$$D_{xoz} \propto \{[(1 - A) \cos(kH_1 \sin \theta) + 2B \cos \alpha]^2 + [(1 + A) \sin(kH_1 \sin \theta) + 2B \cos \alpha]^2\} \cdot \sin^2 \theta \quad (1)$$

$$D_{yo z} \propto [(1 - A) \cos(kH_1 \cos \varphi) + 2B \cos(kd \sin \varphi) \cos \alpha]^2 + [(1 + A) \sin(kH_1 \cos \varphi) + 2B \cos(kd \sin \varphi) \cos \alpha]^2 \quad (2)$$

When height  $H_1$  and distance  $d$  between  $I_2$  and  $I_3$  are kept fixed, suitably arranging the phase ( $\alpha$ ) and magnitudes ( $A$  and  $B$ ) of the current can obtain high directivity and FTBR values along the  $z$ -axis. In the HFSS model, the aforementioned parameters ( $\alpha$ ,  $A$  and  $B$ ) are affected by the meanderline-shaped slots. By properly tuning the length of the slots, the currents on the slot-modified reflector can achieve good magnitudes and phases, which will lead to a desired large FTBR value [11].

An effective length of the meanderline-shaped slots can be obtained by

$$L_{eff} = L_1 + 2L_2 + L_3 + L_4 - 2W_s = 0.25\lambda_0 \quad (3)$$

Based on the effective length of the meanderline-shaped slots, the antenna can achieve a good FTBR of 17 dB at the operating frequency. As depicted in Fig. 4, four straight short slots on the sides of the reflector are designed to further enlarge the FTBR from 17 dB to 19 dB.

### 2.2. Operating Principle of Wide Bandwidth

As well known, the input resistance of the driven dipole decreases gradually to zero as height  $H_1$  between the driven and reflector decreases to a small proportion of its operating wavelength. When  $H_1 = 0.04\lambda_0$  with the proposed slotted reflector, the impedance matching of the proposed antenna will deteriorate terribly. To solve this problem, a director divided into two ladder-like [12] segments is placed above the driven dipole with the same height  $H_2$  of  $0.04\lambda_0$ . With strong mutual coupling between the driver and director, the radiation impedance can be matched with the feeding input impedance very well, leading to a relatively wide bandwidth.

To better understand the effect of the director on antenna matching,  $S$ -parameter is simulated under varied height  $H_2$  between the driven and director as shown in Fig. 5. The simulated  $S$ -parameter of the model without director is also given for comparison in Fig. 5. The simulated plot without director is similar to the plot of the model which has a director with a height  $H_2 = 27$  mm ( $0.2\lambda_0$ ). Both of them have only one resonant frequency at 2.12 GHz. As height  $H_2$  decreases, it is obviously found that a second resonance point is produced. When  $H_2 = 6$  mm ( $0.04\lambda_0$ ), a good impedance bandwidth can be achieved from 2.05 GHz to 2.43 GHz since the second resonant frequency is obtained at 2.4 GHz. Fig. 6 depicts the currents on the antenna to further study the effects of the height  $H_2$  at 2.4 GHz. In comparison with  $H_2 = 27$  mm ( $0.2\lambda_0$ ), the director attains larger currents at 2.4 GHz when  $H_2 = 6$  mm ( $0.04\lambda_0$ ). Obviously, the currents on the director cause it to act as an additional resonant element to the second resonance.

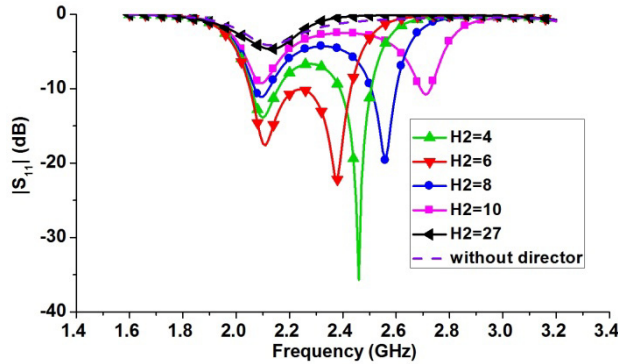


**Figure 5.** Simulated  $|S_{11}|$  variation versus  $H_2$ .

Figure 7 gives the effects of the ladder director parameters on the Yagi antenna performance. When one parameter is studied, the others are kept fixed as shown in Table 1. As shown in Fig. 7(a), when  $L_{do} = 0$ , i.e., the two ladders are not overlapping with each other, the second resonance is not obvious. This further explains that the overlapping region can increase mutual coupling, which contributes much to the antenna matching. By varying the ladder length  $L_{di}$  from 31 to 35 mm, the plots in Fig. 7(b) show that the second resonant frequency shifts down caused by the increased physical dimension. By controlling the overlapping region and length of each ladder, the appropriate impedance matching can be achieved within a wide band.

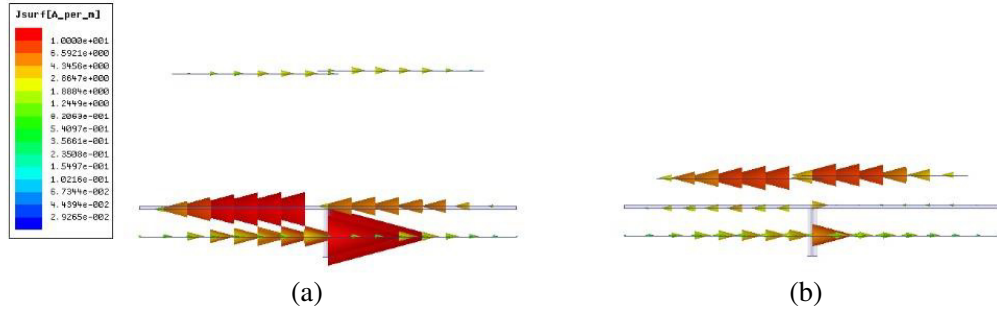


**Figure 6.** Simulated current distributions with varied height  $H_2$  at 2.4 GHz. (a)  $H_2 = 27$  mm, (b)  $H_2 = 6$  mm.

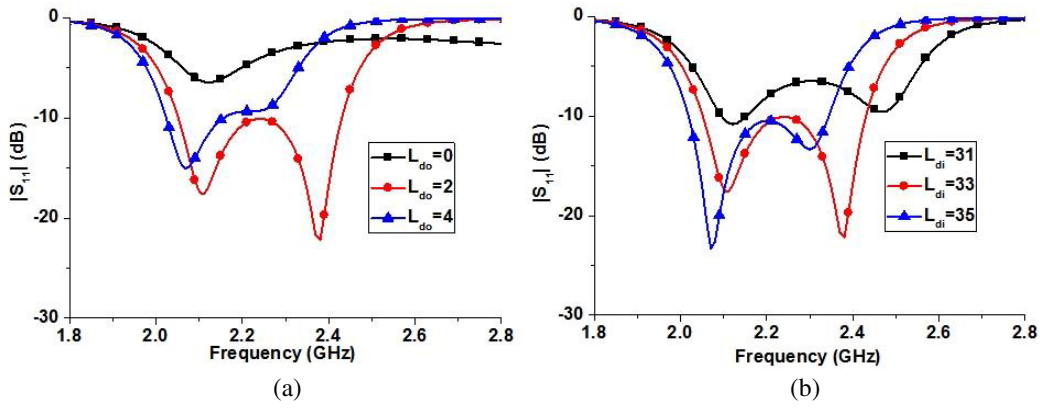


**Figure 7.** Simulated  $|S_{11}|$  variation versus  $L_{do}$  and  $L_{di}$ . (a)  $L_{do}$  ( $L_{di} = 33$  mm), (b)  $L_{di}$  ( $L_{do} = 2$  mm).

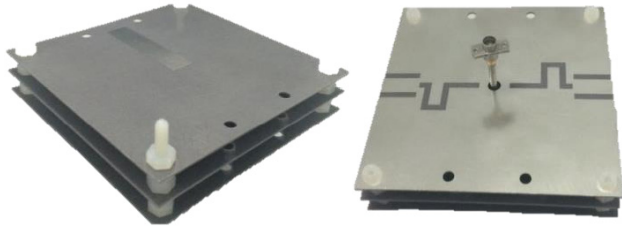


**Figure 8.** The photograph of the fabricated antenna.

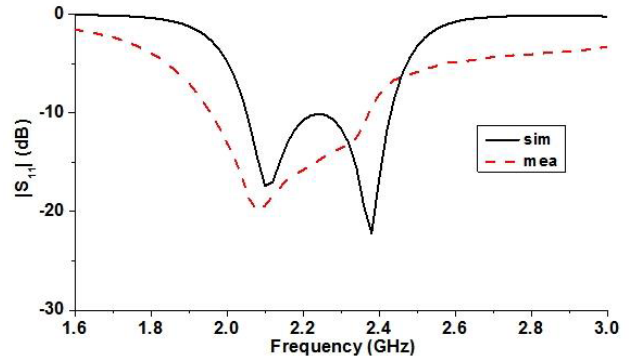


**Figure 9.** Simulated and measured  $|S_{11}|$  as a function of frequency.

### 3. RESULTS

To verify the above design, the proposed compact wideband Yagi antenna is simulated using the HFSS simulation software and fabricated in this section. A photograph of the fabricated Yagi is displayed in Fig. 8. A 50- $\Omega$  SMA connector is used to feed the driven dipole. The simulated and measured results of  $|S_{11}|$  as a function of frequency are shown in Fig. 9. In the band of 1.95–2.4 GHz (2%), the proposed Yagi antenna achieves the measured results of  $|S_{11}| < -10$  dB. It can be seen that a slight difference

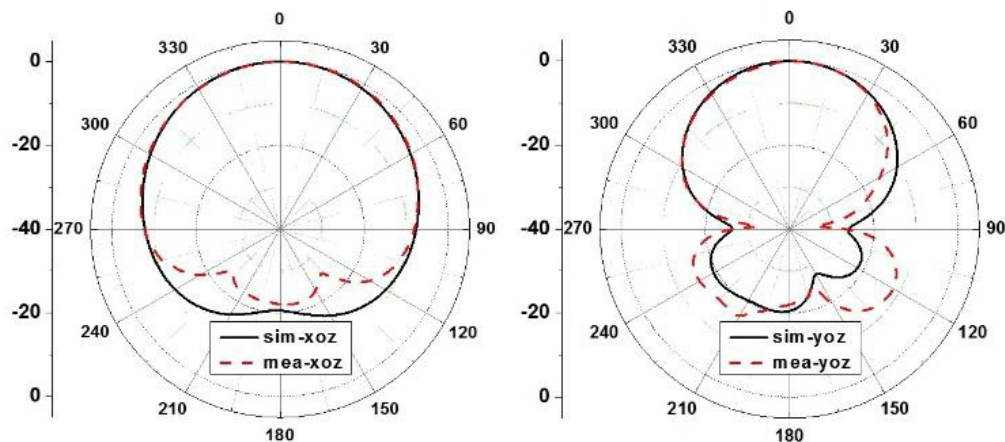


**Figure 10.** Simulated and measured radiation patterns at 2.2 GHz.

exists between the simulated and measured  $S$ -parameters due to the mounting holes in the fabricated model. In the desired band of 17.2%, they agree well with each other. Fig. 10 displays the simulated and measured radiation patterns in the  $xoz$ -plane and  $yozy$ -plane at the central frequency 2.2 GHz. It is noted that the measured FTBR is greater than 22 dB, validating the proposed design.

#### 4. CONCLUSION

In this paper, a compact stacked Yagi antenna is proposed with bandwidth enhancement. Six slots are etched on the reflector ground to reduce the size of the antenna and improve the front-to-back ratio (FTBR). For increasing the bandwidth of the compact stacked Yagi antenna, a ladder-like director is properly designed. By tuning the height between the driven dipole and the director, and the parameters of the ladder director, the bandwidth is expanded to 17.2% with a further diminishing size. As shown in both simulation and measurement, the proposed compact Yagi antenna can be better applied in aircraft communication where wide bandwidth and limited space are needed.

#### REFERENCES

1. Kramer, O., T. Djerfafi, and K. Wu, "Very small footprint 60 GHz stacked Yagi antenna array," *IEEE Trans. Antennas Propag.*, Vol. 59, No. 9, 3204–3210, Sep. 2011
2. Chen, Z. N., Y. Juan, X. M. Qing, and W. Q. Che, "Enhanced radiation from a horizontal dipole closely placed above a PEC ground plane using a parasitic strip," *IEEE Trans. Antennas Propag.*, Vol. 64, No. 11, 4868–4871, Nov. 2016
3. Piersanti, S., F. D. Paulis, A. Orlandi, S. Connor, B. Archambeault, P. Dixon, M. A. Khorrani, and J. L. Drewniak, "Electric dipole equations in very-near-field conditions for electromagnetic shielding assessment — Part II: wave impedance, reflection, and transmission," *IEEE Trans. Electromagn. Compat.*, Vol. 59, No. 4, 1203–1209, Aug. 2017.
4. Yuan, B. and X. Wang, "Multi-objective optimization of double-folded Yagi antenna using genetic algorithms," *Proc. Computational Intelligence and Software Engineering Conf.*, Dec. 2010.
5. Liu, H., Y. Liu, and S. X. Gong, "A novel dual-polarized slot Yagi-Uda array antenna with high gain and low profile," *Proc. International Workshop on Electromagnetics: Applications and Student Innovation Competition*, May 2016.
6. Wang, Q. Q., Z. P. Qian, W. Q. Cao, Y. S. Zhang, and K. Li, "60 GHz stacked Yagi magneto-electric dipole antenna with wideband and high gain properties," *Proc. Communication Problem-Solving Conf.*, 454–457, Oct. 2015.

7. McMichael, I. T., A. I. Zaghoul, and M. S. Mirotznik, "A method for determining optimal EBG reflection phase for low profile dipole antennas," *IEEE Trans. Antennas Propag.*, Vol. 61, No. 5, 2411–2417, May 2013.
8. Best, S. R. and D. L. Hanna, "Design of a broadband dipole in close proximity to an EBG ground plane," *IEEE Antennas Propag. Mag.*, Vol. 50, No. 6, 52–64, Dec. 2008.
9. Huang, Y., A. De, Y. Zhang, T. K. Sarkar, and J. Carlo, "Enhancement of radiation along the ground plane from a horizontal dipole located close to it," *IEEE Antennas Wireless Propag. Lett.*, Vol. 7, 294–297, 2008.
10. Lim, W. G., H. S. Jang, and J. W. Yu, "New method for back lobe suppression of microstrip patch antenna for GPS," *Proc. 40th Eur. Microw. Conf.*, 679–682, Sep. 2010.
11. Tang, M. Ch. and R. W. Ziolkowski, "Efficient, high directivity, large front-to-back-ratio, electrically small, near-field-resonant-parasitic antenna," *IEEE Access*, Vol. 1, 16–28, 2008.
12. Lu, L., K. X. Ma, F. Y. Meng, and K. S. Yeo, "Design of a 60-GHz Quasi-Yagi antenna with novel ladder-like directors for gain and bandwidth enhancements," *IEEE Antennas Wireless Propag. Lett.*, Vol. 15, 682–685, 2016.